




Microenvironment-induced restoration of cohesive growth associated with focal activation of P-cadherin expression in lobular breast carcinoma metastatic to the colon

Malte Gronewold^{1*}, Isabel Grote¹, Stephan Bartels¹ , Henriette Christgen¹, Leonie D Kandt¹, Maria Jose Brito², Gábor Csemi³, Maximilian E Daemrich⁴, Franz Fogt⁵, Burkhard M Helmke⁶, Natalie ter Hoeve⁷, Corinna Lang-Schwarz⁸, Michael Vieth⁸, Axel Wellmann⁹, Elna Kuehnle¹⁰, Ulf Kulik¹¹, Gesa Riedel¹², Tanja Reineke-Plaass¹, Ulrich Lehmann¹, Thijs Koorman⁷ , Patrick WB Derksen⁷, Hans Kreipe¹ and Matthias Christgen¹ 

¹Institute of Pathology, Hannover Medical School, Hannover, Germany

²Pathology and Breast Unit, Champalimaud Foundation, Lisboa, Portugal

³Department of Pathology, University of Szeged, Szeged, Hungary

⁴Group Practice for Pathology Schweinfurt, Schweinfurt, Germany

⁵Pennsylvania Hospital – Penn Pathology and Laboratory Medicine, Philadelphia, PA, USA

⁶Elbe Klinikum Stade – Institut für Pathologie, Stade, Germany

⁷Department of Pathology, University Medical Center Utrecht, Utrecht, The Netherlands

⁸Klinikum Bayreuth – Institut für Pathologie, Bayreuth, Germany

⁹Institute of Pathology Celle, Celle, Germany

¹⁰Clinic for Obstetrics and Gynecology the Neonatology, Hannover Medical School, Hannover, Germany

¹¹Department of General, Visceral, and Transplant Surgery, Hannover Medical School, Hannover, Germany

¹²Department of Immunology and Rheumatology, Hannover Medical School, Hannover, Germany

*Correspondence to: Matthias Christgen, Institute of Pathology, Hannover Medical School, Carl-Neuberg-Str. 1, 30625 Hannover, Germany.

E-mail: christgen.matthias@mh-hannover.de

Abstract

Invasive lobular carcinoma (ILC) is a special breast cancer type characterized by noncohesive growth and E-cadherin loss. Focal activation of P-cadherin expression in tumor cells that are deficient for E-cadherin occurs in a subset of ILCs. Switching from an E-cadherin deficient to P-cadherin proficient status (EPS) partially restores cell–cell adhesion leading to the formation of cohesive tubular elements. It is unknown what conditions control EPS. Here, we report on EPS in ILC metastases in the large bowel. We reviewed endoscopic colon biopsies and colectomy specimens from a 52-year-old female (index patient) and of 18 additional patients (reference series) diagnosed with metastatic ILC in the colon. EPS was assessed by immunohistochemistry for E-cadherin and P-cadherin. *CDH1*/E-cadherin mutations were determined by next-generation sequencing. The index patient's colectomy showed transmural metastatic ILC harboring a *CDH1*/E-cadherin p.Q610* mutation. ILC cells displayed different growth patterns in different anatomic layers of the colon wall. In the tunica muscularis propria and the tela submucosa, ILC cells featured noncohesive growth and were E-cadherin-negative and P-cadherin-negative. However, ILC cells invading the mucosa formed cohesive tubular elements in the intercryptal stroma of the lamina propria mucosae. Inter- cryptal ILC cells switched to a P-cadherin-positive phenotype in this microenvironmental niche. In the reference series, colon mucosa infiltration was evident in 13 of 18 patients, one of which showed intercryptal EPS and conversion to cohesive growth as described in the index patient. The large bowel is a common metastatic site in ILC. In endoscopic colon biopsies, the typical noncohesive growth of ILC may be concealed by microenvironment-induced EPS and conversion to cohesive growth.

Keywords: lobular breast cancer; cadherin switching; growth pattern; variants; tumor-stroma-interaction

Received 17 August 2023; Revised 30 November 2023; Accepted 21 December 2023

No conflicts of interest were declared.

Parts of this work were presented at the International Lobular Breast Cancer Symposium (ILC Symposium, Utrecht, June 20, 2022) and at Lower Saxony's educational seminars for board-certified pathologists ('Rätsselecke', Hannover, April 23, 2022).

© 2024 The Authors. *The Journal of Pathology: Clinical Research* published by The Pathological Society of Great Britain and Ireland and John Wiley & Sons Ltd.

This is an open access article under the terms of the [Creative Commons Attribution-NonCommercial-NoDerivs](https://creativecommons.org/licenses/by-nc-nd/4.0/) License, which permits use and distribution in any medium, provided the original work is properly cited, the use is non-commercial and no modifications or adaptations are made.

Introduction

Invasive lobular carcinoma (ILC) is a special histological breast cancer (BC) type [1,2]. ILC is defined by noncohesive growth patterns, such as dissociated growth and ‘single files’, as described by Foote, Stewart, Fechner, Azzopardi, and others [3–7]. In most cases, noncohesive growth is due to somatic mutation of the *CDH1* gene, which encodes the epithelial cadherin (E-cadherin) cell adhesion molecule [8–11]. The typical immunophenotype of ILC is E-cadherin-negative, estrogen receptor (ER)-positive, progesterone receptor (PR)-positive, HER2-negative, and GATA3-positive [1]. Focal activation of placental cadherin (P-cadherin) expression in E-cadherin-negative tumor cells occurs in a subset of ILCs (<10% of cases) [12]. We have termed the switching from an E-cadherin deficient to a P-cadherin proficient status as EPS, which provides a short abbreviation. EPS partially restores cell–cell adhesion and facilitates the formation of focal cohesive tubules in ILC [12]. We have recently provided a molecular characterization of such tumors, which we have named ILC with tubular elements [12]. We consider this as a morphological variant of ILC, which is related to EPS [1,12,13].

P-cadherin is an alternative classical cell adhesion molecule and is encoded by the *CDH3* gene. From an evolutionary perspective, *CDH3* arose by duplication of *CDH1* [14]. *CDH1* and *CDH3* both map to chromosome 16q22.1 and share 66% homology [15]. P-cadherin expression is rare in luminal (i.e. ER-positive and/or PR-positive) BC (5–23% of cases) [12,16,17]. *In vitro* cell models have shown that, in the absence of E-cadherin, P-cadherin alone partially rescues epithelial adherens junctions (AJs), relocates β -catenin to the cell membrane, and partially re-establishes cell–cell adhesion [17]. It is currently unknown what conditions control EPS, which appears to be a transient phenomenon in ILC [1].

ILC is associated with widespread metastatic dissemination [18,19]. Metastases may be detected at primary diagnosis or as late as >20 years after disease onset [20–24]. Common sites include bone, skin, orbit, ovary, stomach, and the large bowel [20–25]. Patients with intestinal ILC involvement are mostly treated with palliative endocrine and/or chemotherapy [21]. Palliative surgery is rarely considered for therapy, for instance, to prevent ileus [21]. The histology of ILC metastases to the colon has not been studied systematically, so far. The literature is limited to clinical reports [21,26]. Here, we provide a histologic study of 19 patients diagnosed with ILC metastases in the

colon. We show that, in a subset of cases, ILC cells acquire an EPS phenotype and switch to cohesive growth, when they invade the lamina propria mucosae. Awareness of EPS may be helpful for the interpretation of colon biopsies from ILC patients.

Materials and methods

Tumor specimens

Tumor tissues included formalin-fixed paraffin-embedded (FFPE) specimens from 19 patients with ILC metastatic to the colon (Table 1). The index patient was diagnosed with metastatic ILC at the Hannover Medical School (MHH) in 2021. For the index patient, FFPE specimens included (i) a core needle biopsy of the left mammary gland, (ii) an endoscopic colon mucosa biopsy, and (iii) a subtotal colectomy specimen. The reference series included 18 additional patients with ILC metastatic to the colon and/or appendix vermiformis. The reference series was compiled from tissues archives of nine institutions from five countries (Germany, Hungary, USA, The Netherlands, and Portugal). All non-MHH archival specimens included in the reference series were transferred to the MHH tissue archive in accordance with local ethical guidelines. The reference series included cases diagnosed between 2004 and 2022. Colectomy specimens were preferred. However, colectomy specimens were rare because surgery is not regularly considered for palliation of intestinal metastases [21]. Biopsy specimens were admitted only if the biopsy size was sufficient for central immunohistochemical re-assessment. Postmortem sections were excluded, due to common autolytic changes. Archival primary breast tumor specimens corresponding to the patients included in the reference series of colon metastases were no longer available at the time of this study. All available information is included in Table 1. Control tissues included normal colon mucosa ($n = 10$, mostly from women treated with hemi-colectomy for endometriosis), ulcerative colitis ($n = 11$), hyperplastic polyps ($n = 10$), and adenomatous polyps ($n = 10$). All specimens were made anonymous for scientific purposes. In addition, informed patient consent was obtained from the index patient. In addition, this retrospective study was approved by the local ethics committee (MHH, Hannover, ID 10166-BO-K-2022).

Immunohistochemistry

All cases were subjected to central immunohistochemistry (IHC) at the MHH. For IHC, 1- μ m thick sections of FFPE

Table 1. Tumor specimens, histologic characteristics

Case		Clinical			Morphology							
Number	ID	Age (years)	Time to met. (years)	Sample type	Histology	Grade	Serosa	Infiltrated layers				Growth pattern
								Musc. propria	Submucosa	Mucosa	Mucosal burden	
Index	HAN-4770 (biopsy)	52	syn	bx	ILC	G2				m	focal	dis, tel ^a
Index	HAN-4947 (colectomy)	52	syn	ce	ILC	G2	s	mp	sm	m	focal	dis, tel ^a
Reference series												
1	HAN-27112	46	meta	ce	ILC	G2	s	mp	sm	m	focal	dis
2	HAN-26773	69	meta	ce	ILC	G3	s	mp	sm	m	bulky	dis, sol
3	HAN-20946	71	meta	bx	ILC	G2				m	focal	dis
4	HAN-15627	71	meta	bx	ILC	G2				m	focal	dis
5	KEC-5662	na	na	ce	ILC	G3	s	mp	sm	m	ulc	dis
6	PEN-2775	47	na	ce	ILC	G2	s	mp	sm	m	focal	dis
7	PEN-4264	55	na	ce	ILC	G2	s	mp	sm	m	ulc	dis
8	PEN-12834	72	na	ce	ILC	G3	s	mp	sm			dis, sf, agg ^b
9	PEN-2914	70	na	ce	ILC	G2	s	mp	sm	m	focal	dis, sf, agg ^a
10	UTR-12548	53	meta (4)	ce	ILC	G2	s	mp	sm	m	ulc	dis
11	STA-15701	83	na	ce	ILC	G3	s					dis, sf
12	STA-2069	76	na	ce	ILC	G2	s					dis, sol
13	SCH-9550	72	meta (16)	ce	ILC	G2	s	mp	sm	m	focal	dis
14	SCH-23981	62	meta (8)	ce	ILC	G2	s	mp	sm	m	focal	dis, sf
15	LIS-5751	62	meta (12)	bx	ILC	G2				m	focal	c, agg ^a
16	BAY-154363	63	na	bx	ILC	G2			sm			dis
17	BAY-61949	82	na	bx	ILC	G2			sm	m	focal	c, tel ^a
18	CEL-9689	82	na	ae	ILC	G2	s	mp				c, agg ^c

ae, appendectomy; agg, aggregates; bx, biopsy; ce, colectomy; dis, dissociated; ILC, invasive lobular carcinoma; m, mucosa; meta, metachronous; mp, tunica muscularis propria; na, not available; sf, single files; sm, tela submucosa; sol, solid; syn, synchronous; tel, tubular elements; ulc, ulceration.

^aTubular elements and/or cohesive aggregates located in the intercryptal stroma of the colon mucosa.

^bAggregates located in the submucosa.

^cAggregates located in the subserosa.

tissue blocks were mounted on superfrost slides (Thermo Fisher Scientific, Rockford, IL, USA). Slides were deparaffinized and rehydrated conventionally and were subjected to immunohistochemical staining on a Benchmark Ultra automated stainer (Ventana, Tucson, AZ, USA). The CC1 mild program was used for antigen retrieval and the ultraView DAB kit (Ventana) for signal detection. Antibodies used for IHC included the monoclonal anti-E-cadherin antibody ECH-6 (1:100, Zytomed, Berlin, Germany) and the monoclonal anti-P-cadherin antibody clone 56 (1:100, BD Transduction Laboratories, Heidelberg, Germany). Further antibodies and scoring methods are included in the supplementary material, Table S1.

Mutational analysis

Extraction of DNA and mutational analyses were performed as described previously [12,27]. In brief, genomic DNA was extracted with the Maxwell RSC DNA FFPE kit (Promega, Madison, WI, USA) on a Maxwell RSC instrument (Promega). DNA was quantified using a Qubit 2.0 fluorometer (Invitrogen, Darmstadt, Germany) and the Qubit dsDNA HS assay kit (Life Technologies, Carlsbad, CA, USA). Next-generation sequencing (NGS)

of the *CDH1* gene was performed with genomic DNA on an Ion S5 system (Life Technologies) using a customized *CDH1* NGS panel designed with Ion AmpliSeq™ designer software (version 5.6). This panel covered the complete protein-coding sequence of the *CDH1* gene (16 exons and 882 codons), the 5'-UTR sequence of exon 1, and the 3'-UTR sequence of exon 16 with 26 amplicons [27]. Mean ($n = 15$) mapped reads per sample was 244.414 (range, 52.438–852.359), and mean depths per base was 6.378 (range, 1.123–23.137). Amplicons passed QC parameters when the amplicon coverage was at least 500, with a minimum of 100 reads per sequencing direction. Variants were required to have an allelic frequency of at least 3% to be considered true positives. Variant annotation was performed with the ANNOVAR analysis software and database tools (<http://www.openbioinformatics.org/annovar>) [28]. BAM files were preanalyzed with the Ion Reporter software (version 5.10.1.0, Thermo Fisher Scientific).

Laser-assisted microdissection

Laser-assisted microdissection was performed as described previously [29]. In brief, serial sections

(5- μ m-thick FFPE tissue sections) were mounted on a poly-L-lysine-coated membrane fixed on a metal frame. After deparaffinization and H&E-staining, carcinoma infiltrates were purified from distinct anatomical regions (lamina propria mucosae and tela submucosa) using a CellCut Plus system (MMI Molecular Machines and Industries AG, Glattbrugg, Switzerland) [29].

Results

Index patient, clinical presentation

A 52-year-old female (referred to as index patient) presented with subileus symptoms. Colonoscopy showed an ill-circumscribed stenosis of the colon transversum and colon descendens. The patient's medical record provided the following information: (i) systemic scleroderma with Raynaud syndrome and antinuclear autoantibodies (ANAs) of the anti-RNA polymerase III type (diagnosed 16 months earlier), (ii) screening mammography without suspicious findings (13 months earlier), and (iii) lobular breast carcinoma (stage cT1b, cN0) diagnosed by ultrasound-guided needle biopsy of the left breast (1 month earlier). The patient had not yet undergone lumpectomy when subileus symptoms developed.

Index patient, endoscopic colon biopsy

A colon mucosa biopsy was taken during colonoscopy. Histologic assessment revealed sparse infiltrates of an adenocarcinoma. Tumor cells formed cohesive tubules in the stroma between colon crypts (Figure 1A). Nuclei were round and rather monomorphic. The cytoplasm was wide and pale to amphophilic. Tumor cells were negative for intestinal differentiation markers (CK20 $-$, CDX2 $-$, and SATB2 $-$) but positive for mammary markers (CK7 $+$, GATA3 $+$, and ER $+$) (Figure 1B). Autochthonous crypts showed the opposite immunophenotype (CK20 $+$, CDX2 $+$, SATB2 $+$ and CK7 $-$, GATA3 $-$, ER $-$) (Figure 1B). Crypts were E-cadherin-positive and P-cadherin-negative, but the tumor cells were E-cadherin-negative and P-cadherin-positive (Figure 1B, lower right). Accordingly, the colon biopsy presented a diagnostic dilemma: Although histomorphology argued against metastatic ILC because of cohesive growth in tubules, immunophenotypic features were consistent with those known for ILC.

Index patient, breast needle biopsy

Next, the index patient's colon biopsy was compared with the breast needle biopsy obtained 1 month earlier.

The breast biopsy displayed classic ILC with small tumor cells arranged in single files (supplementary material, Figure S1). ILC cells were ER-positive, PR-positive, HER2-negative, and E-cadherin-negative and showed minimal or no P-cadherin expression (supplementary material, Figure S1). Hence, histologic comparison did not clearly support an origin of the adenocarcinoma in the colon from the synchronous ILC in the breast. However, tumor cells were E-cadherin-negative in both sites.

Index patient, colectomy specimen

Two days after the onset of subileus symptoms, the index patient was treated by subtotal colectomy. Gross pathology examination showed diffuse thickening of the colon wall and a stenosis 7.5 cm in length. Histology revealed transmural adenocarcinoma infiltrates. The bulk of tumor cells was located in the tunica muscularis propria and in the tela submucosa and displayed a noncohesive growth pattern in dissociated single cells (Figure 2). This growth pattern left no doubts about metastatic ILC. The immunophenotype was also consistent with metastatic ILC (CK7 $+$, GATA3 $+$, ER $+$, and E-cadherin $-$) (Figure 2). However, the histology differed completely from the colon biopsy seen before (Figure 1 versus Figure 2). Thorough examination of multiple FFPE blocks revealed different growth patterns in different anatomic layers of the colon wall. Non-cohesive growth was evident in deep layers, namely in the tela submucosa (Figure 2) and in the tunica muscularis propria (supplementary material, Figure S2). Strikingly, cohesive growth was evident wherever ILC cells invaded the mucosa (Figure 3). In fact, ILC cells formed cohesive aggregates and tubular elements in the stroma of the lamina propria mucosae (i.e. in the stroma between crypts) (Figure 3). Conversion from dissociated to cohesive growth was readily apparent on staining for CK7 (Figure 3). ILC cells also gained a much wider cytoplasm in this microenvironment (Figure 3). IHC demonstrated an EPS phenotype. ILC cells in deep layers were E-cadherin-negative and P-cadherin-negative (Figure 2), but intercryptal ILC cells switched to a P-cadherin-positive immunophenotype (Figure 3). Of note, multiple, separated foci of mucosa infiltration were evident along the thickened colon segment. ILC cells consistently switched to a P-cadherin-positive phenotype and formed tubular elements wherever mucosa infiltration was evident. Overview photomicrographs showing this phenomenon in multiple foci are included in the supplementary material, Figure S3.

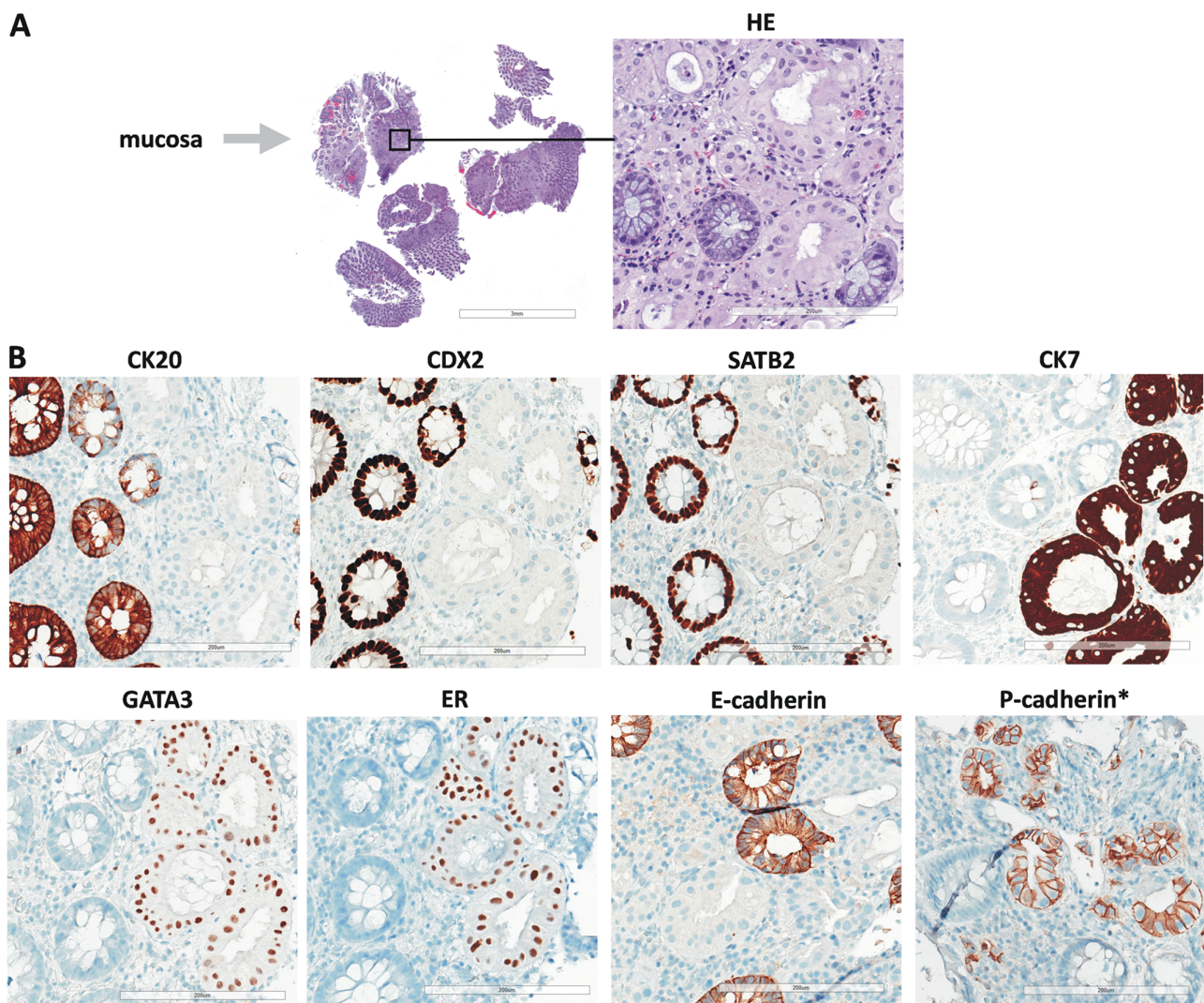


Figure 1. Index patient, endoscopic colon biopsy (ID HAN-4770). (A) Photomicrographs of an H&E-stained section. A submacroscopic view is presented on the left side. The scale bar corresponds to 3.0 mm. Note that the endoscopic biopsy included only mucosa and did not reach into the tela submucosa. Details of the H&E-stained section are presented on the right side ($\times 200$ magnification). The scale bar corresponds to 200 μm . Note that tumor cells form cohesive tubular elements (pale to amphophilic) in the intercryptal stroma between autochthonous colon crypts (basophilic). (B) Photomicrographs of serial sections subjected to immunohistochemical stainings for intestinal differentiation markers (CK20, CDX2, SATB2) and mammary epithelial markers (CK7, GATA3, ER, E-cadherin, P-cadherin). Scale bars correspond to 200 μm . Note that autochthonous crypts are CK20+, CDX2+, SATB2+ and CK7-, GATA3-, ER-, E-cadherin+, P-cadherin-, while cancerous tubular elements are CK20-, CDX2-, SATB2- and CK7+, GATA3+, ER+, E-cadherin-, P-cadherin+. *P-cadherin was stained *ex post*, after the colectomy specimen had already been evaluated.

Loss of E-cadherin is typically accompanied by downregulation of β -catenin protein expression and cytoplasmic or nuclear translocation of p120-catenin [30,31]. EPS partially restores AJ formation and re-establishes membranous β -catenin and p120-catenin expression [12,17]. Accordingly, β -catenin and p120-catenin were assessed by IHC. In deep layers, ILC cells were β -catenin-negative and showed aberrant cytoplasmic

p120-catenin (Figure 2). In the mucosa, however, ILC cells showed restored membranous β -catenin immunoreactivity (Figure 3). Expression of p120-catenin exhibited partially membranous, partially cytoplasmic immunoreactivity. Taken together, the histomorphology and immunohistochemical features confirmed a *bona fide* EPS phenotype of metastatic ILC cells in the intercryptal stroma of the colon mucosa.

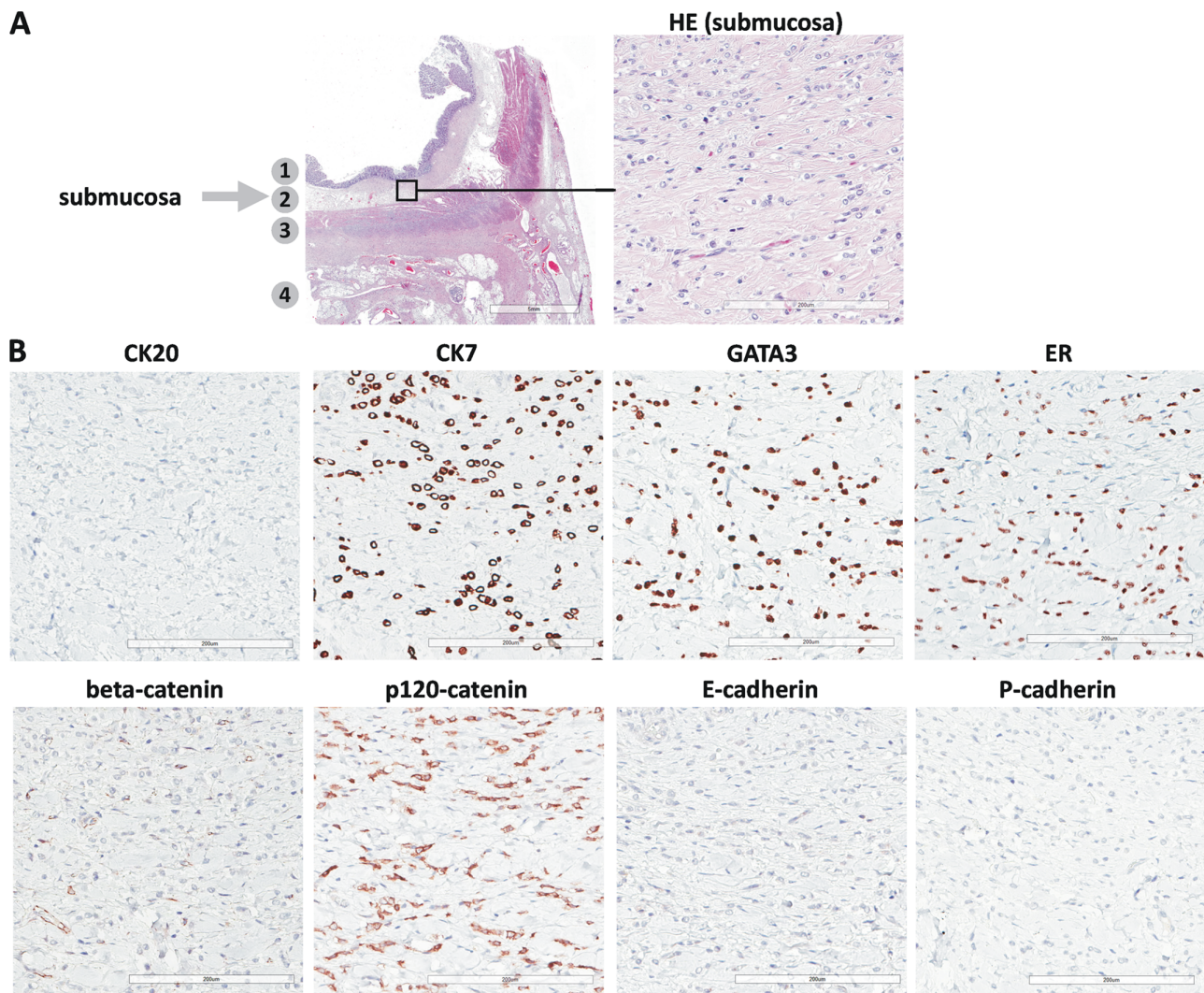


Figure 2. Index patient, colectomy, tela submucosa (ID HAN-4947). (A) Photomicrographs of an H&E-stained section. A submacroscopic view of the colon wall is presented on the left side. The scale bar corresponds to 5.0 mm. Numbers on the left margin annotate anatomic layers of the colon wall: 1, mucosa; 2, tela submucosa; 3, tunica muscularis propria; and 4, connective tissue of the mesenterium and subserosa. Details from the tela submucosa are presented on the right side ($\times 200$ magnification). The scale bar corresponds to 200 μm . Note the noncohesive, dissociated growth pattern. (B) Photomicrographs of serial sections subjected to immunohistochemical analyses for CK20, CK7, GATA3, ER, β -catenin (beta-catenin), p120-catenin, E-cadherin, and P-cadherin. Scale bars correspond to 200 μm . Note that the tumor cells are E-cadherin-negative and P-cadherin-negative.

Index patient, *CDH1* mutations in the breast biopsy and the colectomy

Histologic assessment of the index patient's colectomy suggested a metastasis from ILC. To verify this assumption, we employed the *CDH1*/E-cadherin mutation status as a marker of clonal relatedness [12,27,32]. As expected, identical somatic *CDH1* mutations were detected in the ILC in the breast needle biopsy (p.Q610*, allelic frequency 42%) and in

the adenocarcinoma in the colon (p.Q610*, allelic frequency 38%). Healthy tissue of the index patient showed a wild-type *CDH1* sequence. Cancerous tubular elements isolated from the lamina propria mucosae of the colon by laser-assisted microdissection also harbored the same *CDH1* p.Q610* mutation (supplementary material, Figure S4). Together, this verified that the adenocarcinoma in the colon was indeed derived from the synchronous ILC in the breast.

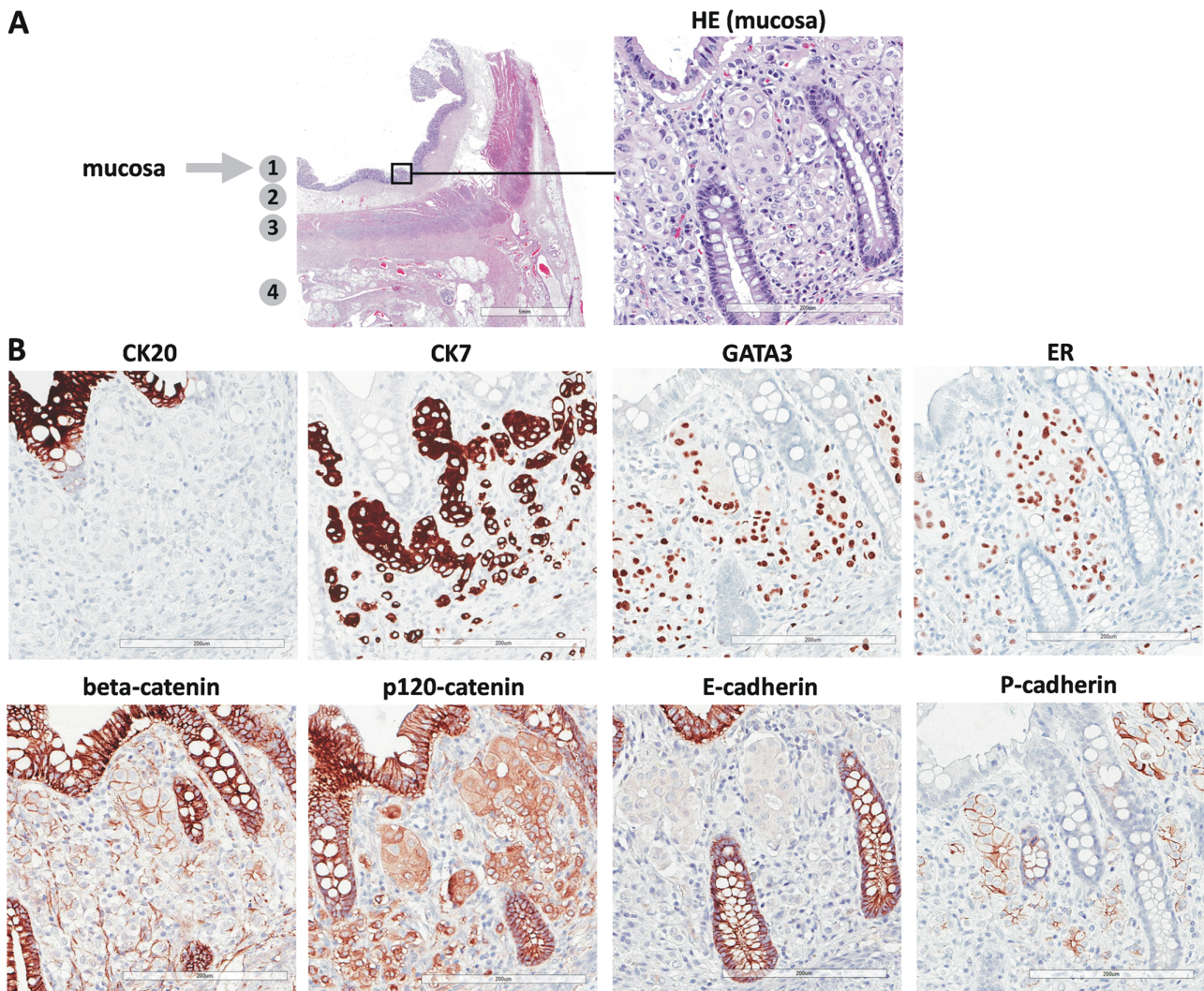


Figure 3. Index patient, colectomy, mucosa (ID HAN-4947). (A) Photomicrographs of an H&E-stained section. A submacroscopic view of the colon wall is presented on the left side (same specimen as shown in Figure 2). The scale bar corresponds to 5.0 mm. Numbers on the left margin annotate anatomic layers of the colon wall: 1, mucosa; 2, tela submucosa; 3, tunica muscularis propria; and 4, connective tissue of the mesenterium and subserosa. Details from the mucosa are presented on the right side ($\times 200$ magnification). The scale bar corresponds to 200 μm . Note the growth in cohesive aggregates and tubular elements. (B) Photomicrographs of serial sections subjected to immunohistochemical analyses for CK20, CK7, GATA3, ER, β -catenin (beta-catenin), p120-catenin, E-cadherin, and P-cadherin. Scale bars correspond to 200 μm . Note that E-cadherin-negative tumor cells switch to a P-cadherin-positive immunophenotype (EPS phenotype).

Control series of normal colon mucosa and various colon lesions

The index patient showed an EPS phenotype in metastatic ILC cells in the colon mucosa. Autochthonous crypts were P-cadherin-negative (Figure 3B). For completeness, we characterized E-cadherin and P-cadherin expression in a control series ($n = 41$ cases) comprising normal colon mucosa specimens, inflammatory, hyperplastic, and neoplastic lesions (supplementary material, Table S2). Normal colon mucosa specimens

were E-cadherin-positive and P-cadherin-negative (10/10 cases), consistent with previous studies [33]. However, discrete P-cadherin expression was noted in sporadic crypts above gut-associated lymphatic tissue (GALT) (supplementary material, Figure S5) [34]. Ulcerative colitis, hyperplastic colon polyps, and adenomatous polyps showed co-expression of E-cadherin and P-cadherin (10/11, 10/10, and 10/10 cases, respectively) (supplementary material, Figure S6). This is in line with the known up-regulation of P-cadherin in the

colon mucosa in response to injury, inflammation, and neoplastic transformation [33,35–38]. GATA3 and CK7 expression were also evaluated in the colon control series. As expected, ulcerative colitis, hyperplastic colon polyps, and adenomatous polyps showed focal upregulation of CK7, but these lesions never showed any immunoreactivity for the mammary epithelial cell marker GATA3 (0/41 cases) (supplementary material, Table S2).

Reference series of colon metastases from ILC

We wondered how often EPS occurs in colon metastases from ILC. Accordingly, we compiled a reference series of colon metastases from ILC (Table 1). Nine institutions from five countries contributed to the reference series. A total of 23 cases were submitted for central re-evaluation. Five cases were excluded due to insufficient tissue size ($n = 2$) or due to re-classification as BC of no special type ($n = 3$). The final reference series included 18 patients. Median patient age was 70 years. Colectomy or appendectomy specimens accounted for 13/18 (72%) cases and endoscopic biopsies accounted for 5/18 (28%) cases. Tumor burden differed interindividually. Mucosa infiltration was evident in 13/18 (72%) cases. Among patients with mucosa involvement, 9/13 (69%) cases showed sparse ILC infiltrates, and 4/13 (31%) cases showed bulky infiltrates or ulceration. All cases (18/18, 100%) were CK7-positive, GATA3-positive, and E-cadherin-negative (Table 2). A total of 15/18 (83%) cases expressed either ER or PR or both hormone receptors, and 3/18 (17%) cases were triple-negative. Deleterious *CDH1* mutations were detected in 9/14 (64%) cases (Table 2). No *CDH1* sequencing results were obtained in 4/18 cases.

EPS was detected in 5/18 (28%) cases (Table 2). EPS occurred either in the subserosa (case 18, ID CEL-9689), or in the tela submucosa (case 8, ID PEN-12834), or in the intercryptal stroma of the mucosa (cases 9, 15, and 17; IDs PEN-2914, LIS-5751, and BAY-61949). One case resembled the index patient (case 17, ID BAY-61949). This large endoscopic biopsy covered mucosa and parts of the tela submucosa (Figure 4). In the submucosa, ILC cells showed noncohesive growth in dissociated single cells (Figure 4A, dashed arrows). In the mucosa, ILC cells formed cohesive aggregates or abortive tubules and gained a wider cytoplasm (Figure 4A, solid arrow). In the submucosa, ILC cells were E-cadherin-negative and P-cadherin-negative (Figure 4B, dashed arrows), but in the mucosa, ILC switched to a P-cadherin-positive immunophenotype (Figure 4B, solid arrow).

Upregulation of P-cadherin restored membranous β -catenin expression (supplementary material, Figure S7). In the other cases with EPS phenotypes, we observed less well-defined aggregates admixed among noncohesive ILC cells (supplementary material, Figures S8–S11). Taken together, EPS occurred in 28% of colon metastases from ILC. Among 13 patients with mucosa infiltration, one case resembled the index patient and showed EPS and conversion to cohesive growth in the intercryptal stroma of the lamina propria mucosae.

Discussion

ILC is a special BC type and is defined by noncohesive growth and E-cadherin loss [1–5]. In a subset of ILCs, EPS partially restores cell–cell adhesion and facilitates the formation of cohesive tubular elements [12]. We have recently provided a molecular characterization of such tumors, which we have named ILC with tubular elements [12]. We consider this as a morphological variant of ILC, which is related to EPS [1,12,13]. It remains unknown whether environmental conditions and which molecular mechanisms control EPS and whether EPS is a transient state of cellular differentiation [1].

EPS becomes clinically relevant if it occurs in metastases. In this constellation, cohesive growth argues against metastatic ILC and raises the possibility of a second malignancy. We have previously reported on an ovarian metastasis from ILC, which showed EPS and tubular elements harboring a *CDH1* p.S9* mutation (case 3 in Christgen *et al* [12]). Originally, this case had been submitted for second opinion consultation to clarify the differential diagnosis between primary ovarian adenocarcinoma and metastatic ILC [12]. This case exemplified that unawareness of EPS may cause considerable diagnostic uncertainty [12]. Here we report a new series of ILC cases, which further underscore the relevance of EPS for clinical diagnostics.

The colon biopsy of the index patient showed an adenocarcinoma, which formed cohesive tubules between colon crypts. Metastatic ILC seemed to be unlikely. A histomorphological comparison of the adenocarcinoma in the colon biopsy with the synchronous ILC in the breast did not support metastatic ILC. However, four lines of evidence established the diagnosis of metastatic ILC. First, the immunophenotype was consistent with metastatic ILC. Second, identical somatic *CDH1*/E-cadherin mutations (p.Q610*) were detected in the colon and the breast. This verified

Table 2. Tumor specimens, immunophenotypic and molecular characteristics

Case Number	ID	IHC										NGS				
		ER	PR	HER2	HER2 (FISH)	Ki67	CK7	GATA3	E-cadherin	P-cadherin	beta-catenin	p120-catenin	CDH1 status	Allelic freq.		
Index	HAN-4770 (biopsy)	pos	na	na	na	<5	pos	pos	neg	fpos	na	na	na			
Index	HAN-4947 (colectomy)	pos	na	1	na	<5	pos	pos	neg	fpos	pos (c/m)	p.0610*	na	38%		
Reference series																
1	HAN-27112	neg	neg	na	na	5	pos	pos	neg	neg	neg	pos (c/n)	p.T580Hfs*4	19%		
2	HAN-26773	pos	pos	na	na	25	pos	pos	neg	neg	neg	pos (c/n)	wt			
3	HAN-20946	pos	neg	1	na	5	pos	pos	neg	neg	neg	pos (c/n)	na			
4	HAN-15627	pos	neg	1	na	5	pos	pos	neg	neg	neg	pos (c/n)	na			
5	KEC-5662	neg	neg	0	na	15	pos	pos	neg	neg	neg	pos (c/n)	na			
6	PEN-2775	pos	neg	1	na	15	pos	pos	neg	neg	neg	pos (c/n)	p.0346Sfs*4	21%		
7	PEN-4264	pos	pos	0	na	15	pos	pos	neg	neg	neg	pos (c/n)	wt			
8	PEN-12834	neg	pos	1	na	15	pos	pos	neg	fpos	fpos	pos (c/n)	p.I600Hfs*11	14%		
9	PEN-2914	pos	pos	0	na	5	pos	pos	neg	fpos	fpos	pos (c/n)	splicing ^a	32%		
10	UTR-12548	pos	pos	0	na	10	pos	pos	neg	neg	neg	pos (c/n)	p.L705Cfs*17	24%		
11	STA-15701	pos	pos	2	neg	25	pos	pos	neg	neg	neg	pos (c/n)	p.M670Gfs*2	22%		
12	STA-2069	pos	pos	0	na	10	pos	pos	neg	neg	neg	pos (c/n)	splicing ^b	33%		
13	SCH-9550	pos	neg	0	na	5	pos	pos	neg	neg	neg	pos (c/n)	p.D569*	12%		
14	SCH-23981	pos	neg	1	na	5	pos	pos	neg	neg	neg	pos (c/n)	wt			
15	LS-5751	pos	neg	1	na	5	pos	pos	neg	fpos	fpos	pos (c/n)	wt			
16	BAY-154363	neg	neg	na	na	35	pos	pos	neg	neg	neg	pos (c/n)	na			
17	BAY-61949	pos	neg	0	na	15	pos	pos	neg	fpos	fpos	pos (c/m)	wt			
18	CEL-9689	pos	neg	1	na	5	pos	pos	neg	fpos	fpos	pos (c/m)	p.O351*	17%		

c/m, partially cytoplasmic and partially membranous immunoreactivity; c/n, partially cytoplasmic and partially nuclear immunoreactivity; FISH, fluorescence *in situ* hybridization; fpos, focally positive immunoreactivity; IHC, immunohistochemistry; na, not available; neg, negative; NGS, next-generation sequencing; pos, positive; wt, wild type.

^aSplice site mutation: c.1565+1G>T.

^bSplice site mutation: c.48+1G>A.

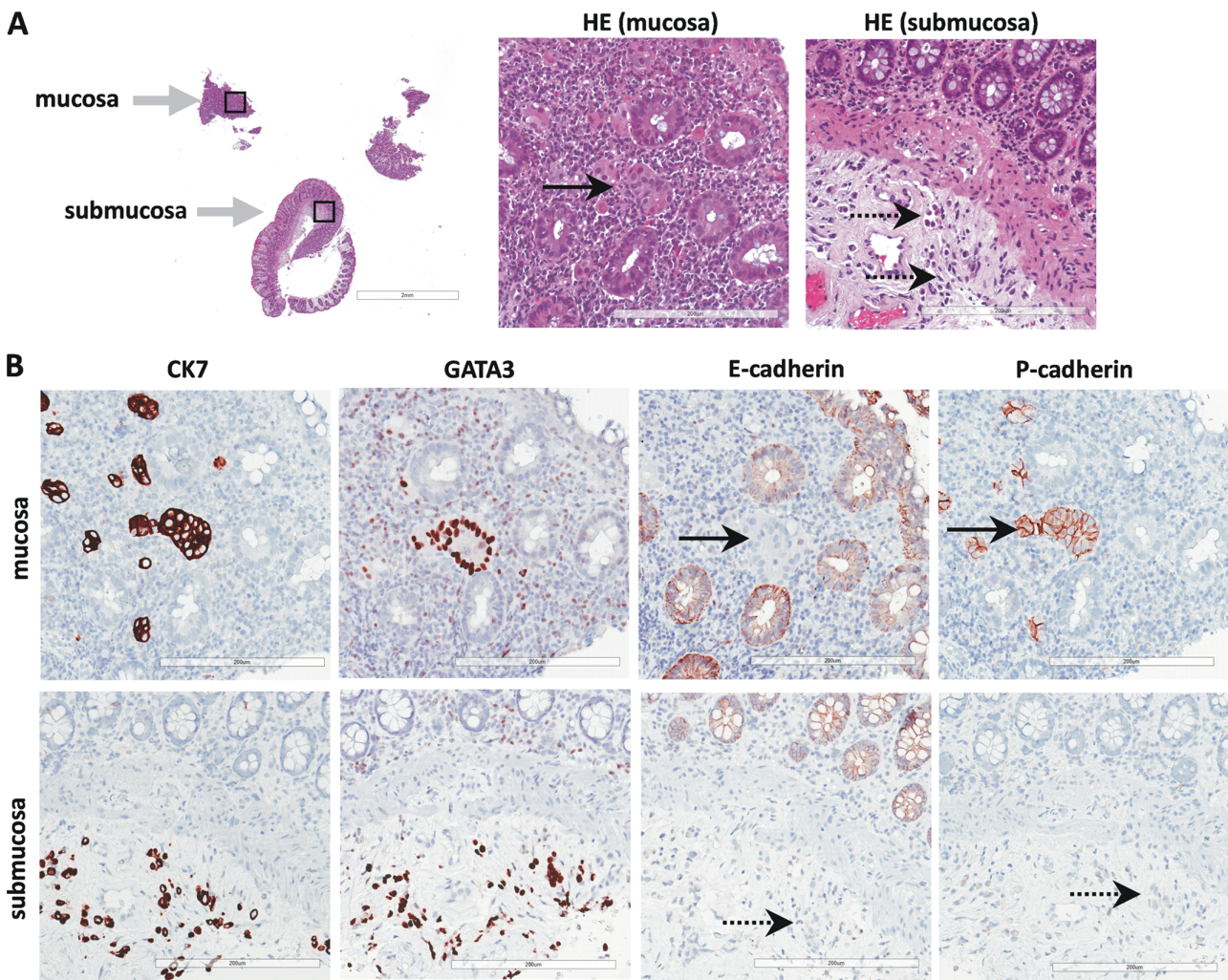


Figure 4. Reference series, patient 17 (ID BAY-61949), endoscopic colon biopsy. (A) Photomicrographs of an H&E-stained section. A submacroscopic view is presented on the left side. The scale bar corresponds to 2.0 mm. Note that the biopsy included not only mucosa, but also fragments of the tela submucosa (lower gray arrow). Details from the mucosa and submucosa are presented on the right side ($\times 200$ magnification). Scale bars correspond to 200 μm . Note that tumor cells form cohesive aggregates in the intercryptal stroma between autochthonous colon crypts (solid arrows, but grow in a dissociated pattern in the tela submucosa (dashed arrows). (B) Photomicrographs of serial sections subjected to immunohistochemical analyses for CK7, GATA3, E-cadherin and P-cadherin. Scale bars correspond to 200 μm . Note that the tumor cells are E-cadherin-negative and P-cadherin-negative in the submucosa (dashed arrows) but switch to a P-cadherin-positive immunophenotype in the mucosa (solid arrow). Note that the tumor cell cluster that appears to be a cohesive aggregate on the H&E-stained sections is a tubular element in the GATA3-stained section level. Further immunohistochemical staining of this specimen (including β -catenin) are presented in supplementary material, Figure S7.

clonal relatedness [12,27]. Third, tubular elements in the colon biopsy showed an EPS phenotype. Fourth, the colectomy revealed that tumor growth was strictly noncohesive in deep layers of the colon wall. EPS and the unusual growth in cohesive tubular elements were limited to foci of mucosa infiltration. Together, this left no doubt about metastatic ILC.

Findings in the index patient hold an interesting biological implication. Of note, EPS and tubular elements

were seen in multiple foci of mucosa infiltration along the colon segment. This suggests an intrinsic competence for EPS in ILC cells. Furthermore, this implies that the intercryptal stroma of the lamina propria mucosae is a permissive microenvironment that can induce EPS in ILC cells. The reference series of ILC metastases partially supported this conclusion. EPS was mostly seen in foci of mucosa infiltration (3/5 cases), and one specimen (case 17) closely resembled

the index patient's metastasis. In fact, case 17 featured conversion to cohesive growth and EPS in the intercryptal stroma. EPS, as described in the index patient, is not a singular finding.

Cases presenting EPS reported in this study also hold a clinical implication. It is not uncommon that endoscopic forceps biopsies fail to grasp deep tissue layers. Accordingly, the tela submucosa is not always represented in colon biopsies [39]. Given that the colon mucosa appears to be a permissive microenvironment for EPS in some cases of ILC, endoscopic biopsies may be prone to sample ILC infiltrates with a growth pattern that is not representative for the bulk of the lesion buried beneath the mucosa. Awareness of EPS in ILC may thus be helpful for colon biopsy interpretation in diagnostic practice. Metastatic ILC must not be excluded when tumor cells grow in cohesive aggregates or tubular elements. This breaks with a longstanding paradigm, but it is necessary to appreciate the morphological plasticity of ILC [1].

Another interesting detail is the comorbidity of the index patient. As mentioned above, the index patient suffered from systemic scleroderma with ANAs of the anti-RNA polymerase III type. This specific form of scleroderma is likely a paraneoplastic disease caused by a direct immune response against tumor neo-antigens [40]. However, neither the primary tumor in the breast nor the metastasis in the colon showed an excess of tumor-infiltrating lymphocytes. At the time of writing of this manuscript, the index patient was alive at 31 months after colectomy, without tumor progression.

Limitations of the present study included the descriptive approach and the limited number of colectomy specimens with ILC metastases included in the reference series. However, this was related to the fact that subtotal colectomy is not always considered for palliation of metastatic BC. Experimental cell and/or animal models are needed to further dissect how the intercryptal microenvironment activates P-cadherin expression in ILC cells.

Taken together, the large bowel is a common metastatic site in lobular breast carcinoma. In endoscopic colon mucosa biopsies, the typical noncohesive growth of lobular breast carcinoma may be concealed by microenvironment-induced EPS in classical ILC cells and conversion to cohesive growth.

Acknowledgements

This study was supported by a grant from the German Cancer Aid to MC, SB, and HK (grant ID: 70112954).

Author contributions statement

This study was designed by MC, PWBD, HK and MG. LK, HC and MC performed the central immunohistochemical staining. LK, IG, SB and UL carried out mutational analyses. MC, MG and HK performed the central histology re-review. All authors contributed to data collection, data analysis and interpretation. MC, MG and HK wrote the manuscript. All authors reviewed and approved the final manuscript version.

Data availability statement

All available data are included in the text, figures and tables.

References

- Christgen M, Cserni G, Floris G, *et al.* Lobular breast cancer: histomorphology and different concepts of a special spectrum of tumors. *Cancers (Basel)* 2021; **13**: 3695.
- Christgen M, Steinemann D, Kuhnle E, *et al.* Lobular breast cancer: clinical, molecular and morphological characteristics. *Pathol Res Pract* 2016; **212**: 583–597.
- Foote FW, Stewart FW. Lobular carcinoma in situ: a rare form of mammary cancer. *Am J Pathol* 1941; **17**: 496.1–496.3.
- Fechner RE. Infiltrating lobular carcinoma without lobular carcinoma in situ. *Cancer* 1972; **29**: 1539–1545.
- Martinez V, Azzopardi JG. Invasive lobular carcinoma of the breast: incidence and variants. *Histopathology* 1979; **3**: 467–488.
- Allison KH, Brogi E, Ellis IO, *et al.* *WHO Classification of Tumours Editorial Board. Breast Tumours*. International Agency for Research on Cancer: Lyon, 2019.
- Shin SJ, Desmedt C, Kristiansen G, *et al.* *Invasive Lobular Carcinoma Breast Tumours* (5th edn). International Agency for Research on Cancer: Lyon, 2019; 114–118.
- Berx G, Cleton-Jansen AM, Nollet F, *et al.* E-cadherin is a tumour/invasion suppressor gene mutated in human lobular breast cancers. *EMBO J* 1995; **14**: 6107–6115.
- Derksen PW, Liu X, Saridin F, *et al.* Somatic inactivation of E-cadherin and p53 in mice leads to metastatic lobular mammary carcinoma through induction of anoikis resistance and angiogenesis. *Cancer Cell* 2006; **10**: 437–449.
- Desmedt C, Zoppoli G, Gundem G, *et al.* Genomic characterization of primary invasive lobular breast cancer. *J Clin Oncol* 2016; **34**: 1872–1881.
- de Groot JS, Ratze MA, van Amersfoort M, *et al.* alphaE-catenin is a candidate tumor suppressor for the development of E-cadherin-expressing lobular-type breast cancer. *J Pathol* 2018; **245**: 456–467.
- Christgen M, Bartels S, van Lutikhuizen JL, *et al.* E-cadherin to P-cadherin switching in lobular breast cancer with tubular elements. *Mod Pathol* 2020; **33**: 2483–2498.

13. Christgen M, Kandt LD, Antonopoulos W, et al. Inter-observer agreement for the histological diagnosis of invasive lobular breast carcinoma. *J Pathol Clin Res* 2022; **8**: 191–205.
14. Gallin WJ. Evolution of the “classical” cadherin family of cell adhesion molecules in vertebrates. *Mol Biol Evol* 1998; **15**: 1099–1107.
15. Paredes J, Correia AL, Ribeiro AS, et al. P-cadherin expression in breast cancer: a review. *Breast Cancer Res* 2007; **9**: 214.
16. Turashvili G, McKinney SE, Goktepe O, et al. P-cadherin expression as a prognostic biomarker in a 3992 case tissue microarray series of breast cancer. *Mod Pathol* 2011; **24**: 64–81.
17. Ribeiro AS, Sousa B, Carreto L, et al. P-cadherin functional role is dependent on E-cadherin cellular context: a proof of concept using the breast cancer model. *J Pathol* 2013; **229**: 705–718.
18. Ferlicot S, Vincent-Salomon A, Medioni J, et al. Wide metastatic spreading in infiltrating lobular carcinoma of the breast. *Eur J Cancer* 2004; **40**: 336–341.
19. Chen Z, Yang J, Li S, et al. Invasive lobular carcinoma of the breast: a special histological type compared with invasive ductal carcinoma. *PLoS One* 2017; **12**: e0182397.
20. El-Hage A, Ruel C, Afif W, et al. Metastatic pattern of invasive lobular carcinoma of the breast—emphasis on gastric metastases. *J Surg Oncol* 2016; **114**: 543–547.
21. Montagna E, Pirola S, Maisonneuve P, et al. Lobular metastatic breast cancer patients with gastrointestinal involvement: features and outcomes. *Clin Breast Cancer* 2018; **18**: 401–405.
22. DiPiro PJ, Tirumani SH, Cruz GP, et al. Lobular breast cancer: patterns of intraabdominal metastatic spread on imaging and prognostic significance. *Abdom Radiol (NY)* 2019; **44**: 362–369.
23. Raap M, Antonopoulos W, Dammrich M, et al. High frequency of lobular breast cancer in distant metastases to the orbit. *Cancer Med* 2015; **4**: 104–111.
24. Blohmer M, Zhu L, Atkinson JM, et al. Patient treatment and outcome after breast cancer orbital and periorbital metastases: a comprehensive case series including analysis of lobular versus ductal tumor histology. *Breast Cancer Res* 2020; **22**: 70.
25. Chuang AY, Watkins JC, Young RH, et al. Lobular carcinoma of the breast metastatic to the ovary: a clinicopathologic study of 38 cases. *Am J Surg Pathol* 2022; **46**: 179–189.
26. Maharajh S, Capildeo K, Barrow M, et al. Case report of metastatic breast cancer mimicking ileal Crohn’s disease. *Int J Surg Case Rep* 2021; **87**: 106408.
27. Christgen M, Bartels S, van Luttikhuisen JL, et al. Subclonal analysis in a lobular breast cancer with classical and solid growth pattern mimicking a solid-papillary carcinoma. *J Pathol Clin Res* 2017; **3**: 191–202.
28. Wang K, Li M, Hakonarson H. ANNOVAR: functional annotation of genetic variants from high-throughput sequencing data. *Nucleic Acids Res* 2010; **38**: e164.
29. Jonigk D, Golpon H, Bockmeyer CL, et al. Plexiform lesions in pulmonary arterial hypertension composition, architecture, and microenvironment. *Am J Pathol* 2011; **179**: 167–179.
30. de Leeuw WJ, Berx G, Vos CB, et al. Simultaneous loss of E-cadherin and catenins in invasive lobular breast cancer and lobular carcinoma in situ. *J Pathol* 1997; **183**: 404–411.
31. Schackmann RC, van Amersfoort M, Haarhuis JH, et al. Cytosolic p120-catenin regulates growth of metastatic lobular carcinoma through Rock1-mediated anoikis resistance. *J Clin Invest* 2011; **121**: 3176–3188.
32. Christgen M, Bruchhardt H, Hadamitzky C, et al. Comprehensive genetic and functional characterization of IPH-926: a novel CDH1-null tumour cell line from human lobular breast cancer. *J Pathol* 2009; **217**: 620–632.
33. Jankowski JA, Bedford FK, Boulton RA, et al. Alterations in classical cadherins associated with progression in ulcerative and Crohn’s colitis. *Lab Invest* 1998; **78**: 1155–1167.
34. Morbe UM, Jorgensen PB, Fenton TM, et al. Human gut-associated lymphoid tissues (GALT); diversity, structure, and function. *Mucosal Immunol* 2021; **14**: 793–802.
35. Milicic A, Harrison LA, Goodlad RA, et al. Ectopic expression of P-cadherin correlates with promoter hypomethylation early in colorectal carcinogenesis and enhanced intestinal crypt fission in vivo. *Cancer Res* 2008; **68**: 7760–7768.
36. Hardy RG, Brown RM, Miller SJ, et al. Transient P-cadherin expression in radiation proctitis: a model of mucosal injury and repair. *J Pathol* 2002; **197**: 194–200.
37. Hardy RG, Tselepis C, Hoyland J, et al. Aberrant P-cadherin expression is an early event in hyperplastic and dysplastic transformation in the colon. *Gut* 2002; **50**: 513–519.
38. Sanders DS, Perry I, Hardy R, et al. Aberrant P-cadherin expression is a feature of clonal expansion in the gastrointestinal tract associated with repair and neoplasia. *J Pathol* 2000; **190**: 526–530.
39. Wei XB, Gao XH, Wang H, et al. More advanced or aggressive colorectal cancer is associated with a higher incidence of “high-grade intraepithelial neoplasia” on biopsy-based pathological examination. *Tech Coloproctol* 2012; **16**: 277–283.
40. Joseph CG, Darrah E, Shah AA, et al. Association of the autoimmune disease scleroderma with an immunologic response to cancer. *Science* 2014; **343**: 152–157.

SUPPLEMENTARY MATERIAL ONLINE

Figure S1. Index patient, breast needle biopsy

Figure S2. Index patient, colectomy, muscularis propria

Figure S3. Index patient, colectomy, mucosa at multiple sites

Figure S4. Index patient, laser microdissection and *CDH1* sequencing

Figure S5. P-cadherin expression in the normal colon mucosa

Figure S6. E-cadherin and P-cadherin expression in inflammatory, hyperplastic and neoplastic colon lesions

Figure S7. Reference series, case 17, further IHC analyses

Figure S8. Reference series, case 8

Figure S9. Reference series, case 9

Figure S10. Reference series, case 15

Figure S11. Reference series, case 18

Table S1. Antibodies and ICH scoring methods

Table S2. GATA3, CK7, E-cadherin and P-cadherin expression in normal colon and colonic lesions